EXPERIMENTAL STUDY ON BEHAVIORS OF THE TRAPEZOID CONNECTORS OF THE INVERTED T-SHAPED STEEL WITH NOTCHED WEB FOR A NOVEL COMPOSITE BEAM

Li Guo-qiang [1, 2,*], Li Liang [2] and Li Xianhui [2]

[1] *State Key Laboratory for Disaster Reduction in Civil Engineering, Tongji University, Shanghai 200092, People's Republic of China*
[2] *College of Civil Engineering, Tongji University, Shanghai 200092, People's Republic of China*
**(Corresponding author: E-mail: gqli@tongji.edu.cn)*

ABSTRACT: An innovative steel-concrete composite beam with embedding the notched web of the inverted T-shaped steel into the concrete slab is introduced in this paper. The behaviors of the trapezoid connectors of the notched web of the inverted T-shaped steel for the composite beam are experimentally investigated. Firstly, the shear behavior of the connectors is investigated through the tests on ten push-out specimens, and a formula on the base of the test results is proposed to estimate the ultimate shear capacity of the trapezoid connectors. Then the pull-out behavior is studied through tests on six specimens, and the comparisons between pull-out and shear capacities are conducted. Next, the local compressive behavior is studied through tests on four local compressive specimens, and an equation on local compressive capacity of the connectors is proposed on the base of the test results. Finally, testes are conducted on eight specimens to investigate the punch behavior of the connectors, and a formula on punch capacity of the connectors is recommended. According to the experimental results, the trapezoid connectors may promise the reliability of the connection between the concrete slab and the inverted T-shaped steel beam, and the formulas proposed can be practically used to estimate the shear, local compressive and punch capacities of the trapezoid connectors for the novel composite beam.

Keywords: Steel-concrete composite beam; T-shaped steel; push-out specimens; trapezoid connectors

1. INTRODUCTION

The conventional composite beam is composed of a steel beam with H-shaped section and a concrete slab [1-4], and headed studs are used as shear connectors to combine the steel beam and the concrete slab together, as shown in Figure 1(a). In H-shaped steel concrete composite beam, the top flange of the steel beam is at the vicinity of the neutral axis of the section, its stress level is low and the material is not fully used under sagging moment [5]. If the top flange of the steel beam is removed and the isosceles trapezoid notch is cut at the top of web to work as the shear connectors, the steel and headed studs can be saved, as shown in Figure 1(b). The inverted T-shaped steel-concrete composite beam is mainly made up of the steel component with inverted T-shaped section and concrete slab, generally designed to bear sagging moment.

Comparing with the H-shaped steel-concrete composite beam [6-11], the following advantages are found in the inverted T-shaped steel-concrete composite beam:

(1) The top flange of H-shaped steel beam is removed, which would reduce about 20% of steel consumption;

(2) The headed studs are replaced by trapezoid connectors, and the welding process of headed studs is avoided;

(3) Two T-shaped steel beams can be made by cutting along a trapezoid path on the web of one H-shaped steel beam, which would accelerate the pace of construction, as shown in Figure 2.

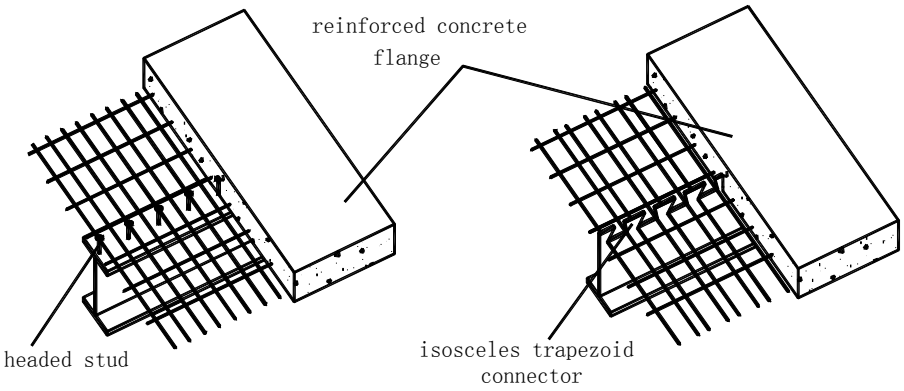

(a) H-shaped Steel-concrete Composite Beam (b) Inverted T-shaped Steel-concrete Composite beam

Figure 1. Steel-concrete Composite Beam with Different Connectors

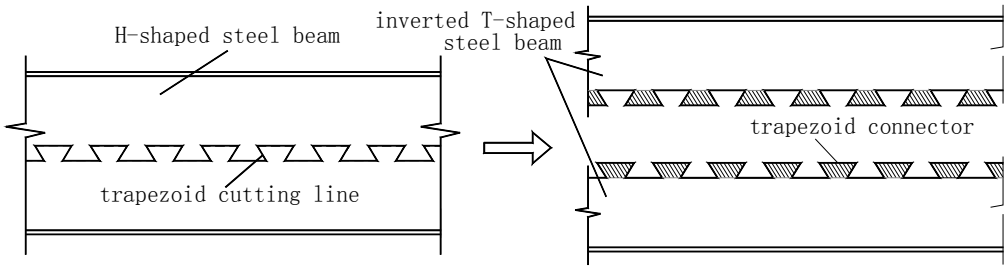

Figure 2. Construction Process of the Inverted T-shaped Steel Beams

For proper design and use of the novel composite beam, the behaviors of the trapezoid connectors of the inverted T-shaped steel with notched web needs to be clearly identified. For this purpose, a series of tests are conducted on behavior of the connection of the specimens to investigate the shear, pull-out, local compression and punch behavior. According to the test results, formulas for estimating the shear, local compressive and punch capacities of the connectors are proposed.

2. PUSH-OUT TEST

2.1 Specimens and Test Set-up

The shear behavior between concrete slab and steel beam may be studied through push-out tests. To study the shear performance of the trapezoid connectors for the novel composite beam, tests are conducted on 10 push-out specimens. Each specimen is composed by an H-shaped steel component, two pieces of connecting plates and two blocks of concrete slabs. One edge of the connecting plate is welded on the flange of the H-shaped steel component, and the other edge is embedded into the concrete slab. A 50mm wide gap is retained between the end of concrete slab and the steel component, as shown in Figure 3.

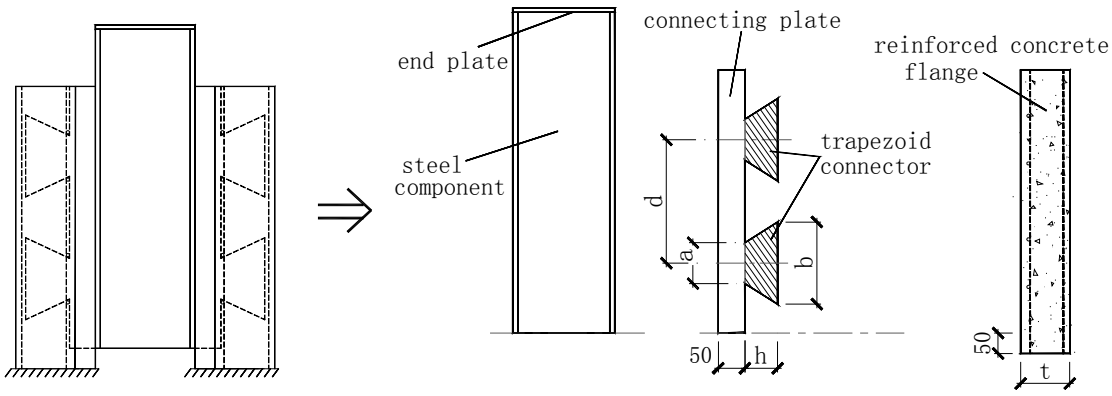

(a) Push-out Specimen (b) Components of the Push-out Specimen

Figure 3. Components of the Push-out Specimen

Settle the specimen vertically on the loading equipment, and apply vertical load on the top of the steel component, as shown in Figure 4. The slip increases with the increasing of the shear between concrete slab and steel component. The shear-slip curves are obtained by recording the vertical load and the slip at every load step.

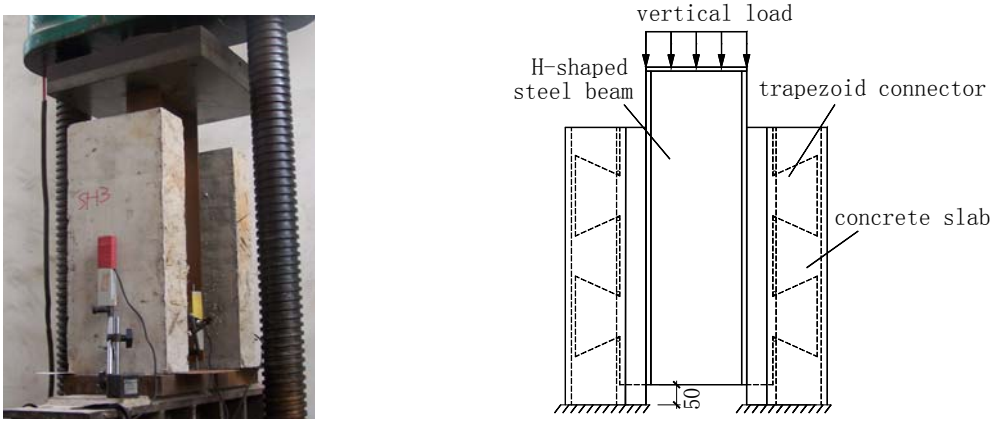

(a) Photo of the Test Set-up (b) Description of the Test Set-up

Figure 4. Push-out Specimen Settled on Loading Device

In order to study the influence of different parameters, 10 specimens are divided into 5 groups, and the 2 specimens in one group are all the same to consider the discreteness of the test results. The specimens SH1～SH6 are designed to study the influence of the strength grade of concrete; the specimens SH5～SH10 are designed to study the influence of dimension of the trapezoid connector, the thickness of the concrete slab and the reinforcement ratio. The details of the specimens are shown in Figure 5～Figure 7. The parameters of the specimens are listed in Table 1.

Table 1. Parameters of Push-out Specimens

No.	Specimen	f_{cu} (N/mm^2)	t (mm)	Dimension of the trapezoid connector				d (mm)	ρ (%)	L (mm)
				t_w (mm)	h (mm)	a (mm)	b (mm)			
1	SH1,SH2	27.5	120	10	80	100	200	300	0.56%	840
2	SH3,SH4	42.5	120	10	80	100	200	300	0.56%	840
3	SH5,SH6	34.2	120	10	80	100	200	300	0.56%	840
4	SH7,SH8	34.2	150	12	110	100	200	300	0.70%	840
5	SH9,SH10	34.2	100	8	60	60	160	240	0.84%	740

In Table 1, f_{cu} is the cubic compressive strength of concrete; t is the thickness of reinforced concrete flange; t_w is the thickness of the connecting plate; h is the height of trapezoid connector; a is the width of lower side of the trapezoid connector; b is the width of the upper side of trapezoid connector; d is the distance between the middle lines of adjacent connectors; ρ is the transverse reinforcement ratio of the concrete slab; and L is the length of the specimen.

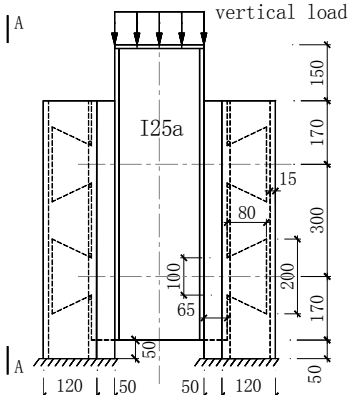

(a) Front Profile

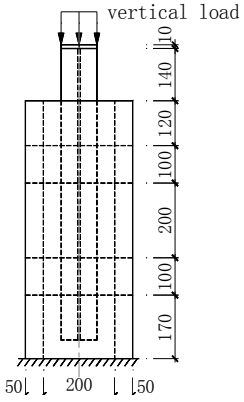

(b) Section A-A

Figure 5. Details of Push-out Specimens SH1~SH6

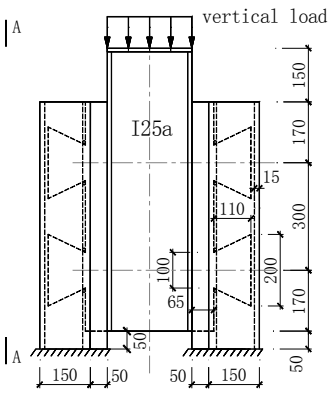

(a) Front Profile

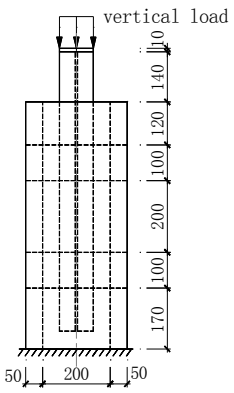

(b) Section A-A

Figure 6. Details of push-out Specimens SH7~SH8

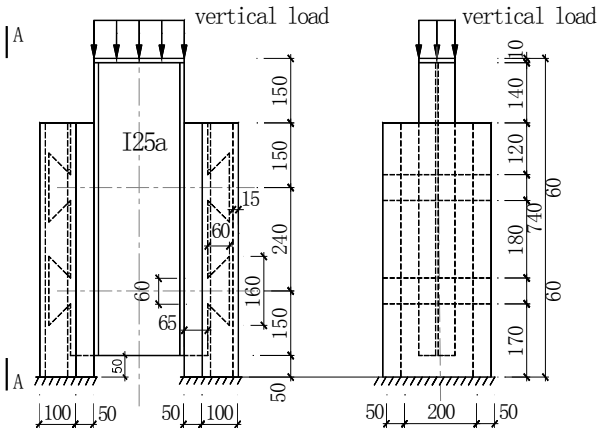

(a) Front profile (b) Section A-A

Figure 7. Details of Push-out Specimens SH9~SH10

The yield strength of the steel for steel component and connecting plate is 345MPa, and the tensile strength is 480MPa. The diameter of reinforcing bars in the concrete slab is 8mm, and the yield strength of the bars is 370MPa.

2.2 Test Phenomenon and Results

When the shear is less than 0.6*Vu* (*Vu* is the ultimate shear capacity of the specimen), there is no crack observed on the concrete slab, which indicates that the specimens remain in elastic state. The elastic modulus and compressive capacity of concrete is much less than that of steel, when the shear reaches 0.6~0.7*Vu*, some transverse cracks are firstly observed on the concrete slab, as shown in Figure 8(a). With the further increasing of the shear, some longitudinal cracks emerge on the concrete slab in the direction of the shear force, and simultaneously accompanied by the sound of the concrete cracking. With the development of the cracks, the shear resisted by concrete is transmitted to the transverse reinforcement and longitudinal cracks interconnect with each other, and the excellent ductility is observed with the increasing of the longitudinal slip. Finally, vertical splitting damage takes place on the concrete slab, as shown is Figure 8(b) and Figure 9 (a). After the tests, there is no damage observed on the trapezoid connectors as the concrete slab is removed, as plotted is Figure 9(b).

(a) The Transverse Cracks on the Side Profile (b) The Longitudinal Cracks on the Front Profile

Figure 8. Lateral and Vertical Cracks of Push-out Specimens during the Test

(a) Longitudinal Cracks on the Concrete Slab (b) Steel Component after the Removal of Concrete

Figure 9. The Failure Conditions of Different Parts after Test

The shear-slip curves of the specimens are shown in Figure 10. It can be seen that non-linear characteristic of the shear-slip curve is very obvious. Though there is no obvious yield plateau on the shear-slip curve, the ductility of the connectors for shear-resistance is fine.

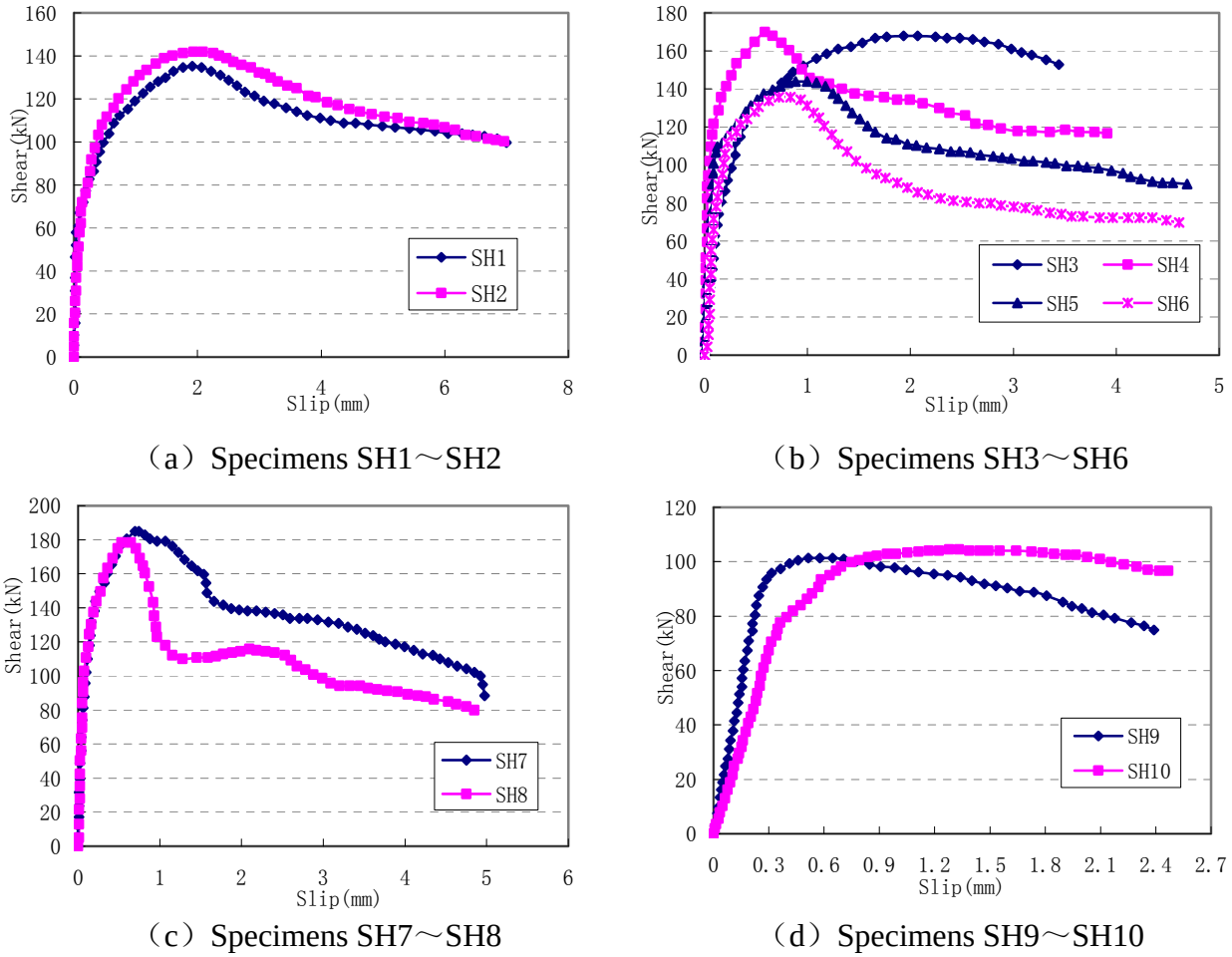

（a）Specimens SH1～SH2

（b）Specimens SH3～SH6

（c）Specimens SH7～SH8

（d）Specimens SH9～SH10

Figure 10. Shear-slip Curves of Push-out Specimens

The main results of the push-out tests are shown in Table 2. According to the test results of specimens SH1～SH6, the shear capacity increases with the improvement of the strength of concrete, but the ductility decreases on the contrary. In the light of the results of the specimens SH5～SH10, the shear capacity increases with the increase of thickness and height of trapezoid connector.

Table 2. Main Results of Push-out Tests

Specimen	Cracking load(kN)	ultimate load(kN)	Cracking slide(mm)	ultimate slide(mm)	Specimen	Cracking load(kN)	ultimate load(kN)	Cracking slide(mm)	ultimate slide(mm)
SH1	98.50	135.20	0.31	1.85	SH6	105.60	135.80	0.25	0.79
SH2	100.70	140.60	0.35	1.92	SH7	120.10	185.10	0.15	0.75
SH3	110.50	165.20	0.40	1.50	SH8	122.80	180.10	0.18	0.56
SH4	112.20	170.40	0.21	0.65	SH9	90.10	105.60	0.11	1.90
SH5	110.10	140.20	0.40	1.12	SH10	83.60	110.40	0.11	1.50

2.3 Estimation of Ultimate Shear Capacity

According to the test results, and referring to the formula of the shear capacity of the steel studs for steel-concrete beams [12], the equation for estimating the ultimate shear capacity of the trapezoid connector can be formulated as:

$$N_v^c = 0.85t_w^2\sqrt{E_c f_c} + 57.25 \quad (1)$$

where E_c is the elastic modulus of concrete (N/mm^2); f_c is the design value of strength of concrete (N/mm^2); and t_w is the thickness of trapezoid connector (mm). It should be pointed out that the effectiveness of the Eq. 1 is based on the limitation that the height of the trapezoid connector, *h*, is no less than 6 times of its thickness, *t*, according to the test phenomenon and results. The comparisons between measured and predicted values are tabulated in Table 3.

Table 3. Comparison between Measured and Predicted Values

Specimen	SH1	SH2	SH3	SH4	SH5	SH6	SH7	SH8	SH9	SH10
Measured Cracking load(kN)	98.50	100.70	110.50	112.20	110.10	105.60	120.10	122.80	90.10	83.60
Predicted cracking capacity (kN)	99.31	99.31	124.22	124.22	112.92	112.92	137.42	137.42	92.88	92.88
Relative error	0.8%	1.4%	11.0%	9.6%	2.5%	6.5%	12.6%	10.6%	3%	7.8%

3. PULL-OUT TEST

3.1 Specimens and Test Set-up

In order to study the pull-out behavior of trapezoid connectors, tests are conducted on 6 pull-out specimens. The specimens are divided into 3 groups, and the specimens in one group are all the same to consider the discreteness of the test results. Each specimen is composed by a block of concrete slab and a piece of connecting plate, as shown in Figure 11. The details about the specimens are tabulated in Table 4.

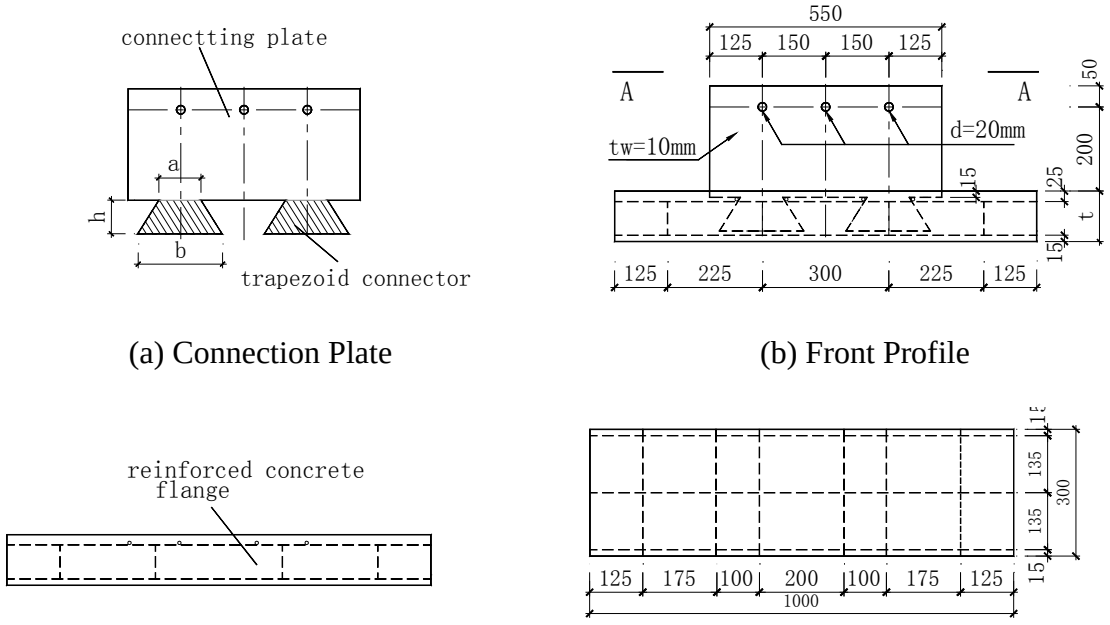

(a) Connection Plate (b) Front Profile

(c) Reinforced Concrete Flange (d) Section A-A

Figure 11. Components of the Pull-out Specimen

Self-balance loading equipment is adopted in the test, and the pull-out force *F* applied by jack can be balanced by two H-shaped steel beams, as plotted in Figure 12. The stiffness of H-shaped steel beam is large enough to pledge the force be uniformly applied on connecting plate.

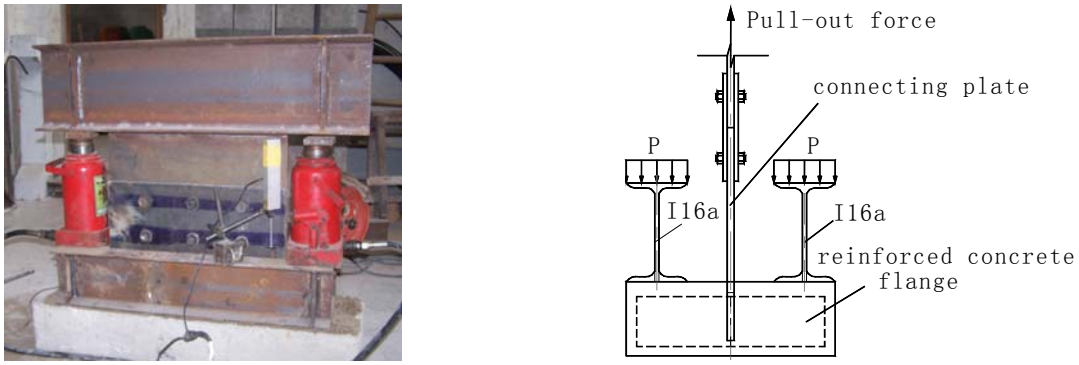

(a) Photo of the Test Set-up (b) Description of the Test Set-up

Figure 12. Test Set-up for the Pull-out Test

Table 4. Parameters of Specimens

Specimen	t (mm)	t_w (mm)	h (mm)	a (mm)	b (mm)	d_i (mm)	ρ	L (mm)
B-1	120	10	80	100	200	8	0.56%	1000
B-2	120	10	80	100	200	8	0.56%	1000
B-3	100	8	60	60	160	8	0.84%	1000
B-4	100	8	60	60	160	8	0.84%	1000
B-5	150	12	110	100	200	10	0.70%	1000
B-6	150	12	110	100	200	10	0.70%	1000

In Table 4, d_i is the diameter of the transverse rebar. The yield strength of the connecting plate is 345MPa, and the tensile strength is 480MPa. The steel of reinforcing bars in the concrete slab is HRB335, and the yield strength is 370MPa. The grade of concrete is C30, and the compression strength is 34.2MPa.

3.2 Test Phenomenon and Results

Monotonic loading is adopted during the pull-out test. While the pull-out force is less than 0.9*Vu* （*Vu* is the ultimate pull-out capacity of the specimen）, there is no crack observed on the concrete slab. While the force arrives at *Vu*, some longitudinal cracks are observed, as shown is Figure 13. The main results of the tests are listed in Table 5, and the force-slip curves of the pull-out tests are plotted in Figure 14. When the displacements are 1.2mm～3.1mm, the pull-out force arrives at the ultimate value.

(a) Specimens B1 and B2 (b) Specimens B3～B6

Figure 13. Failure Phenomenon of the Pull-out Specimens

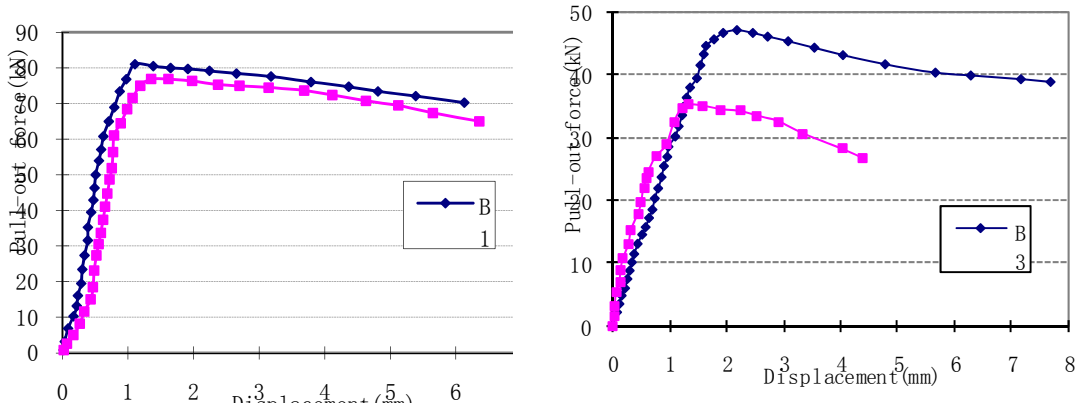

(a) Specimens B1 and B2

(b) Specimens B3 and B4

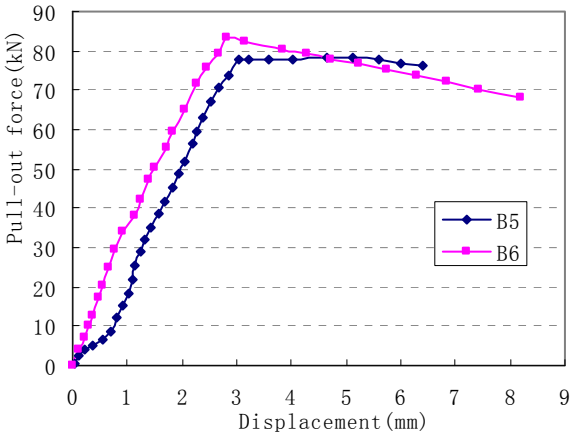

(c) Specimens B5 and B6

Figure 14. Load-displacement Curves of Pull-out Specimens

Table 5. Main Results of Pull-out Tests

Specimen	B-1	B-2	B-3	B-4	B-5	B-6
Failure displacement (mm)	1.2	1.5	2.2	1.3	3.1	2.8
Ultimate pull-out capacity P_u(kN)	81.2	77.1	45.0	36.7	84.9	80.5

3.3 Comparison between Pull-out and Shear Capacities

It is generally believed that the pull-out capacity of the connector is large enough for pull-out resistance of steel-concrete beams if it exceeds 10% of the shear capacity [12]. According to the pull-out capacities of the specimens measured from the tests and the shear capacities estimated with equation (1), the ratios of pull-out capacities to shear capacities of the pull-out specimens are much larger than 0.1, as tabulated in Table 6. Obviously, the pull-out capacity of trapezoid connectors is strong enough and may satisfy the requirement for pull-out capacity of steel-concrete composite beams.

Table 6. Comparison between Pull-out and Shear Capacities

specimen	B-1	B-2	B-3	B-4	B-5	B-6
Pull-out capacity (kN)	81.2	77.1	45.0	36.7	84.9	80.5
Shear capacity (kN)	113	113	92.9	92.9	137	137
Pull-out capacity / shear capacity	0.72	0.68	0.48	0.40	0.62	0.59

4. LOCAL COMPRESSIVE TESTS

4.1 Specimens and Test Set-up

To study the local compressive behavior of the novel composite beam, tests are conducted on 4 local compressive specimens. Each specimen is composed by a T-shaped steel component and a block of concrete slab, as shown in Figure 15. The parameters of the specimens are listed in Table 7. The yield strength of the steel component is 300MPa, and the tensile strength is 380MPa; the yield strength of the reinforcing bar is 314MPa, and the diameter of reinforcing bar is 8mm.

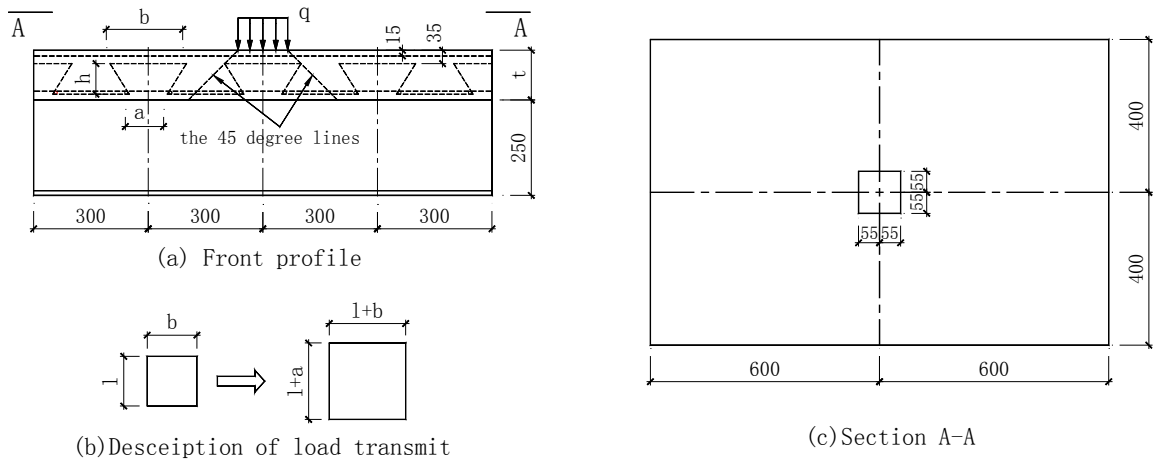

Figure 15. Components of Local Compressive Specimen

Table 7. Parameters of Specimens

Specimen	t (mm)	f_{cu} (N/mm^2)	h (mm)	a (mm)	b (mm)	t_w (mm)	ρ (%)	L (mm)
CQ1	130	31.2	80	100	200	10	0.81%	1000
CQ2	130	24.4	80	100	200	10	0.81%	1000
CQ3	120	31.2	70	80	160	8	0.70%	960
CQ4	120	24.4	70	80	160	8	0.70%	960

Settle the specimen on the test machine, and apply vertical force on top of the slab by jack, as shown in Figure 16. A rectangular steel cushion block is used to transmit the vertical force uniformly on the top of the slab.

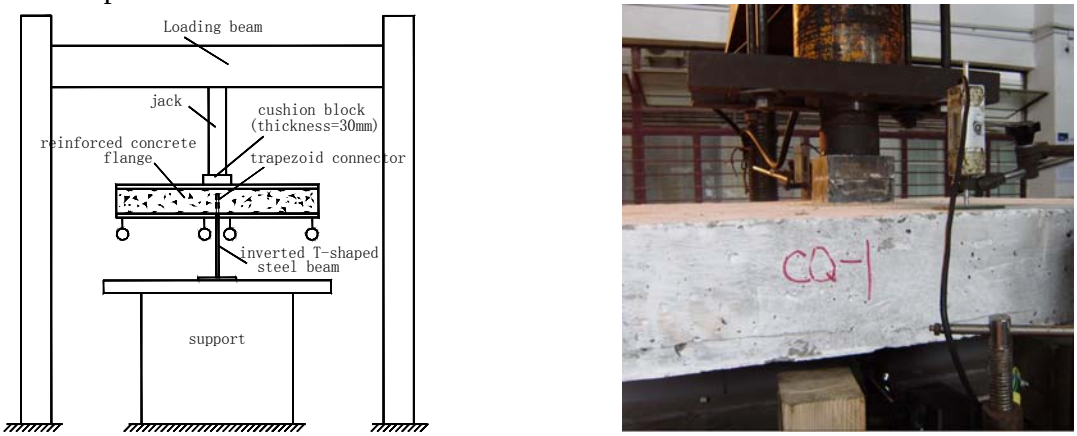

(a) Description of Local Compressive Device (b) Load Device of Local Compressive Test

Figure 16. Test Set-up for the Local Compressive Test

4.2 Test Phenomenon and Results

When the force is less than 0.7*Vu* (*Vu* is the ultimate local compressive capacity of the specimen), there is no crack observed on the concrete slab, which indicates that the specimen is in elastic state. When the force reaches 0.7*Vu*, some transverse cracks are observed in the profile of the concrete slab, as shown in Figure 17(a). With the further increasing of the local pressure, the transverse cracks swiftly interconnect with each other, as shown in Figure 17 (b). When the ultimate local compressive capacity is achieved, there is an obvious groove observed below the cushion block, as shown in Figure 17(c).

(a) Emergence of Initial Lateral Cracks (b) Extension of the Lateral Cracks (c) Local Groove on the Concrete Flange

Figure 17. Phenomenon of the Local Compressive Test

The load-displacement curves of the specimens are plotted in Figure 18. When the force is less than 0.7*Vu*, the relationship between force and displacement is linear; when the force exceeds 0.7*Vu*, the non-linear characteristic of the curve is very obvious. The final failure displacements are tabulated in Table 8.

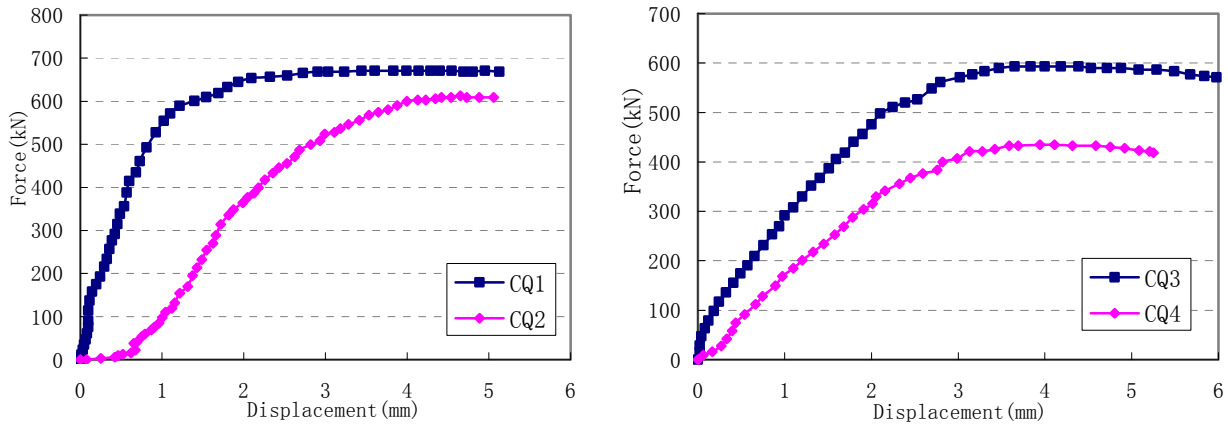

(a) Specimen CQ1 and CQ2 (b) Specimen CQ3 and CQ4

Figure 18. Local Pressure -displacement Curves

Table 8. Main Results of Local Compressive Tests

Specimen	CQ1	CQ2	CQ3	CQ4
Measured failure displacement (mm)	3.93	4.63	3.86	4.02
Measured ultimate local compressive capacity (kN)	670.4	610.9	592.6	433.8
Theoretical value (kN)	640.4	535.3	563.5	445.4
Relative error between theoretical and tested value	4.5%	12.4%	4.9%	2.5%

4.3 Estimation of Ultimate Local Compressive Capacity

From the results of the tests, the local compressive capacity is related to the strength grade of concrete, the area of local compression and the distance from the top of connector to the top surface of concrete slab. Referring to the formula of the local compressive capacity of the steel studs for steel-concrete beams [12], the following formula estimating the ultimate local compressive capacity are obtained as:

$$F_c \le 1.35\beta_c f_{cu}(b+a)(l+a) \tag{2}$$

where β_c is the strength coefficient of the concrete; f_{cu} is the design compressive strength of concrete (N/mm^2); b,l is the width and length of the local pressure (mm); a is the distance from the top of connector to the surface of the concrete slab (mm).

5. PUNCH TEST

5.1 Specimens and Test Set-up

To study the punch behavior of the composite beam with notched web, tests are conducted on 8 punch specimens. Each specimen is composed by an inverted T-shaped steel component and a block of concrete slab. The coincide-work of the steel component and the concrete slab is pledged by trapezoid connectors which are embedded in the concrete slab, as shown in Figure 19. The parameters of specimens are listed in Table 9. The yield strength of the steel is 300MPa, and the tensile strength is 380MPa; the yield strength of the reinforcing bars is 314MPa, and the diameter is 8mm.

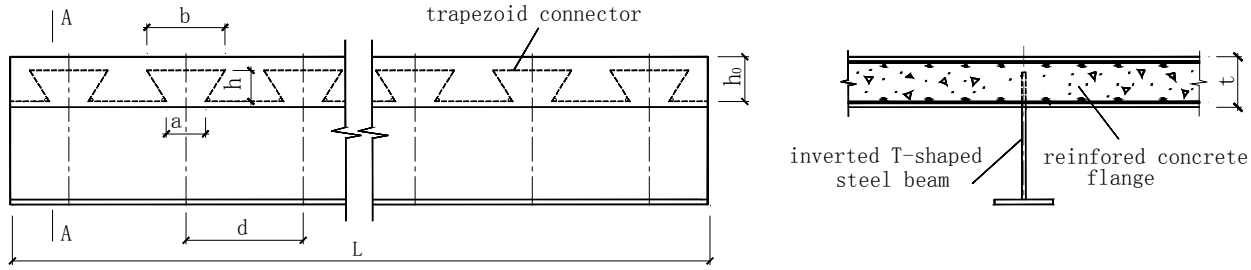

(a) Front Profile (b) Section A-A

Figure 19. Components of Punch Specimens

Table 9. Parameters of the Punch Specimens

Specimen	t (mm)	f_{cu} (N/mm^2)	h (mm)	a (mm)	b (mm)	t_w (mm)	d_i (mm)	ρ	L (mm)	m
CB-1	130	31.2	80	100	200	10	10	0.81%	1200	1
CB-2	130	24.4	80	100	200	10	10	0.81%	1200	1
CB-3	120	31.2	70	80	160	8	8	0.70%	960	1
CB-4	120	24.4	70	80	160	8	8	0.70%	960	1
CQ-5	130	31.2	80	100	200	10	10	0.81%	1200	2.5
CQ-6	130	24.4	80	100	200	10	10	0.81%	1200	2.5
CQ-7	120	31.2	70	80	160	8	8	0.70%	960	2.5
CQ-8	120	24.4	70	80	160	8	8	0.70%	960	2.5

In Table 9, the punch-span ratio m is defined by punch length s divided by effective height h_0 of the concrete slab. Punch length s is the distance from the mid-area of the web to the inner edge of the support, as plotted in Figure 20(b).

The monotonic loading is adopted in the test. Settle the specimen on the test machine, and apply vertical force by jack, as shown in Figure 20. A closed ribbed H-shaped steel beam is adopted to transmit the vertical force uniformly on the top of the steel beam.

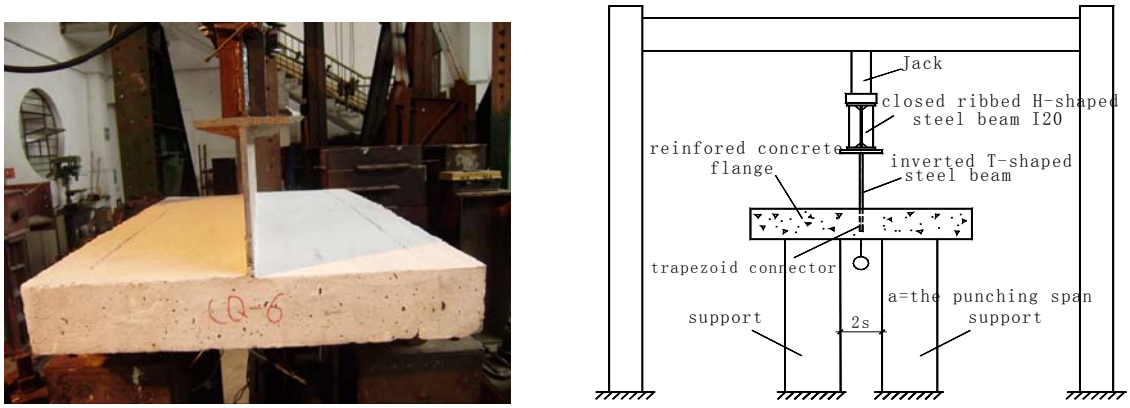

(a) Photo of the Punch Set-up (b) Description of Punch Set-up

Figure 20. Test Set-up for of the Punch Test

5.2 Test Phenomenon and Results

When the punch-span ratios *m* is 1 (specimens CB1～CB4), the failure mode is punch failure. When the punch force is less than 0.3*Vu* (*Vu* is the ultimate punch capacity of the specimen), there is no crack observed on the concrete slab, which indicates that the specimen remains in elastic state. When the punch force reaches 0.4~0.6*Vu*, some cracks are observed on the concrete around the trapezoid connectors, as shown in Figure 21(a). With the further increasing of the punch force, the cracks develop along the 45 angle lines, as shown in Figure 21(b).

(a) Initial Cracks of the Specimen (b) Punch Failure of the Specimen

Figure 21. Test Phenomenon of the Specimens (CB1～CB4)

When the punching-span ratio *m* is 2.5 (specimens CB5～CB8), the failure mode is shear damage. When the punch force is less than 0.6*Vu*, there is no crack observed on the concrete slab. When the punch force reaches 0.6~0.7*Vu*, some cracks are observed, as shown in Figure 22(a). With the increasing of the punch force, apparent bending is observed, and the damage takes place in the concrete slab, as shown in Figure 22(b).

(a) Initial Cracks of the Specimen

(b) Shear-bending Failure of the Specimen

Figure 22. Test Phenomenon of the Specimens (CB5～CB8)

The force-displacement curves of the specimens are shown in Figure 23. When the punch force is less than 0.3～0.5*Vu*, the relationship between force and displacement is linear. While the force exceeds 0.5*Vu*, the concrete slab cracks, the tension stress would transmit from the cracked concrete to reinforcing bars, the stiffness of the specimen reduces rapidly, and the force-displacement curve develops into nonlinear phase. The failure displacements and ultimate punch capacity obtained from the tests are tabulated in Table 10.

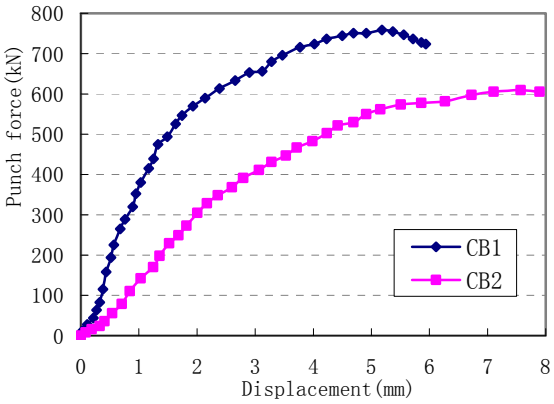

(a) Specimens CB1 and CB2

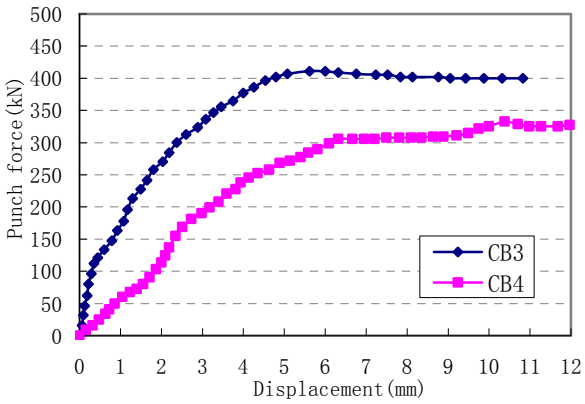

(b) Specimens CB3 and CB4

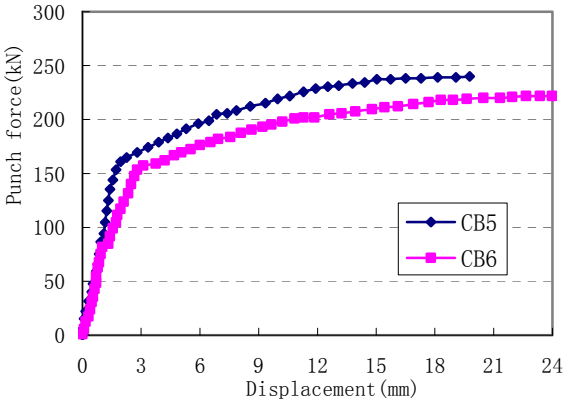

(c) Specimens CB5 and CB6

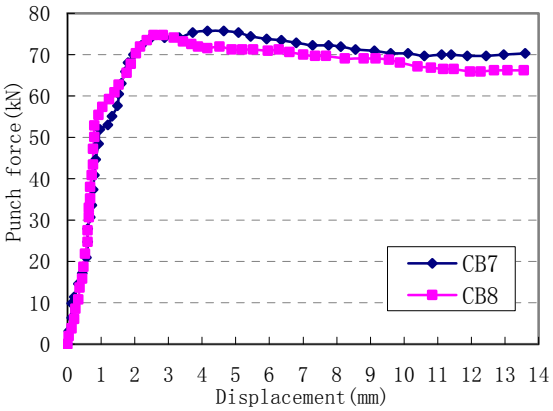

(d) Specimens CB7 and CB8

Figure 23. Punch Force-displacement Curve for Specimens

5.3 Estimation of Ultimate Punch Capacity

In light of the test results, and referring to the formula of the punch capacity for steel-concrete beams [12], the following formula for estimating the ultimate punch capacity is proposed as:

$$F_l \le 0.9\beta_h f_t u_m h_0 \tag{3}$$

where β_h is the factor of the section height; f_t is design tension strength of concrete (N/mm^2); u_m is the total length of the upper and lower punch failure lines (mm); h_0 is the effective height of the section (mm), as shown in Figure 24.

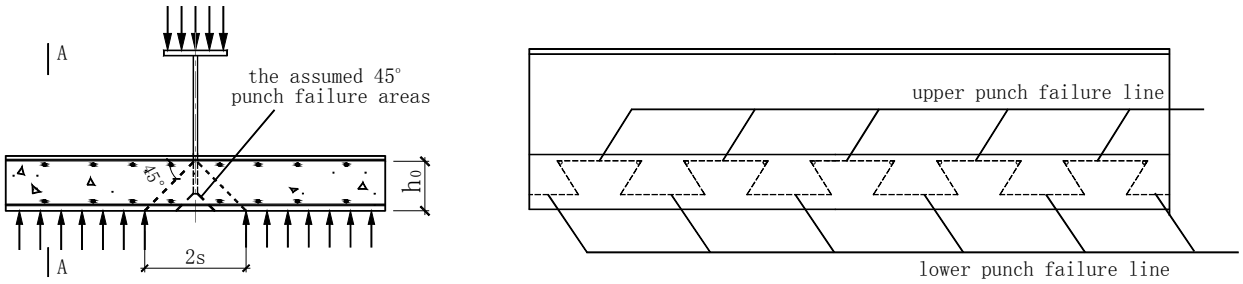

(a) Front Profile (b) Section A-A

Figure 24. Punch Failure Lines

Predicted punch capacities of the tested specimens is listed in Table 10, which match the measured results well. Tests show that the punch capacity of the specimen increases with the improvement of the ultimate compressive strength of concrete f_{cu}.

Table 10. Test Results of the Punch Tests

Specimen	CB-1	CB-2	CB-3	CB-4	CQ-5	CQ-6	CQ-7	CQ-8
Measured failure displacements(mm)	3.12	3.95	5.12	5.86	3.45	3.78	3.2	3.8
Measured ultimate punch capacity P(kN)	652.1	501.6	418.7	312.3	230.5	218.6	76.8	71.6
Predicted punch capacity (kN)	567	458.7	413.3	333.5	No	No	No	No
Relative error	-13%	-8.5%	-1.3%	+6.8%	No	No	No	No
Failure style	Punch	Punch	Punch	Punch	Shear-bending	Shear-bending	Shear-bending	Shear-bending

6. CONCLUSIONS

This paper systematically investigates the push- and pull-out, local compressive and punching behaviors of the trapezoid connectors of the inverted T-shaped steel with notched web through the experimental studies, and the following conclusions are drawn:

(1) The trapezoid connector of the inverted T-shaped steel-concrete composite beam may strongly combine the steel component and concrete slab together, which may pledge concrete slab and steel beam to work commonly.

(2) The elastic modulus and compressive capacity of concrete are much less than that of steel, and there is no damage observed on the trapezoid connectors after the tests compared to the longitudinal slip, even the concrete slab is severely damaged.

(3) The formulas proposed in this paper are based on the test results presented, the reliability of which needs to be checked with further more tests.

ACKNOWLEDGEMENTS

The work reported hereinabove is financially supported by the ministry of science and technology of China through projects SLDRCE08-A-06 and 2006BAJ01B02, which is gratefully acknowledged.

REFERENCES

[1] Newmark, N.M., Siess, C.P. and Viest, I.M., “Test and Analysis of Composite Beams with Incomplete Interaction”, Experimental Stress Analysis, 1951, Vol. 9, No. 6, pp. 896-901.

[2] Johnson, R.P., “Partial-interaction Design of Composite Beams”, The Structural Engineer, 1975, Vol. 3, No. 8, pp. 1-21.

[3] Crisinel, M., “Partial-interaction Analysis of Composite Beams with Profiled Sheeting and Non-welded Shear Connectors”, Journal of Construction Steel Research, 1990, Vol. 15, pp.65-98.

[4] Grant, J.A. and Fisher, J.W., ”Composite Beams with Formed Steel Deck”, Engineering Journal, AISC, 1977, Vol. 14, No. 1, pp. 24-43.

[5] Christopher, H., “Behavior of Composite Bridge Decks with Alternative Shear Connectors”, Journal of Bridge Engineer, 2001, pp. 17-22.

[6] Li, G.Q. and Li, X.H., “Study on a Novel Steel-concrete Composite Beam”, ICASS '09 / IJSSD / IStructE Asia-Pacific Forum Sixth International Conference on Advances in Steel Structures, Nov, 2009.

[7] Galambos, T.V., “Recent Research and Design Developments in Steel and Composite Steel-concrete Structures in USA”, J. Constructional Steel Research, 2000, Vol. 55, No. 1, pp. 289-303.

[8] Roger, G., Slutter, “Flexural Strength of Steel-concrete Composite Beams”, Proceedings of ASCE, Journal of the Structural Division, 1965, Vol. 91, No. 4, pp. 71-99.

[9] Li, X.H. and Li, G.Q., “Study on the Behavior of Embedded Steel-Concrete Composite Beams with Notched Web during Construction Stage”, 9th International Conference on Steel Concrete Composite and Hybrid Structures, Leeds UK, July, 2009.

[10] Brian, Uy, “Application Behavior and Design of Composite Steel-concrete Beams subjected to Combined Actions”, Proceedings of the 9th International Conference on Steel Concrete Composite and Hybrid Structures (ASCCS2009), Leeds, UK, July 2009.

[11] Eurocode 4, “Design of Composite Steel and Concrete Structures, Part 1.1: General Rules and Rules for Buildings”, 1994.

[12] GB50017-2003, “Code for Design of Steel Structures”, Beijing: Chinese Construction Industry Press, 2002.